Science Translational Medicine
AAAS

Gene Therapy Prolongs Survival and Restores Function in Murine and Canine Models of Myotubular Myopathy

Martin K. Childers *et al.*

Sci Transl Med **6**, 220ra10 (2014);
DOI: 10.1126/scitranslmed.3007523

Editor's Summary

Restoring Skeletal Muscle Function

X-linked myotubular myopathy is a fatal disease of skeletal muscle that affects about 1 in 50,000 male births. Patients harbor mutations in the *MTM1* gene and are typically born floppy, with severely weak limb and respiratory muscles. Survival requires intensive support, often including tube feeding and mechanical ventilation, but effective therapy is not available for patients. Gene replacement therapy using adeno-associated viral (AAV) vectors has potential for the treatment of inherited diseases like myotubular myopathy. Therefore, Childers *et al.* tested the effects of a recombinant AAV vector expressing myotubularin in two animal models of myotubularin deficiency: *Mtm1* knockout mice and dogs carrying a naturally occurring *MTM1* gene mutation. Results in both mice and dogs showed that a single intravascular injection of AAV strengthened severely weak muscles, corrected muscle pathology, and prolonged survival. No toxicity or immune response was observed in dogs. These results demonstrate the efficacy of gene replacement therapy for myotubular myopathy in animal models and pave the way to a clinical trial in patients.

Science Translational Medicine (print ISSN 1946-6234; online ISSN 1946-6242) is published weekly, except the last week in December, by the American Association for the Advancement of Science, 1200 New York Avenue NW, Washington, DC 20005.

GENE THERAPY

Gene Therapy Prolongs Survival and Restores Function in Murine and Canine Models of Myotubular Myopathy

Martin K. Childers,[1,2]* Romain Joubert,[3] Karine Poulard,[3] Christelle Moal,[3] Robert W. Grange,[4] Jonathan A. Doering,[4] Michael W. Lawlor,[5,6] Branden E. Rider,[5] Thibaud Jamet,[3] Nathalie Danièle,[3] Samia Martin,[3] Christel Rivière,[3] Thomas Soker,[6] Caroline Hammer,[3] Laetitia Van Wittenberghe,[3] Mandy Lockard,[7] Xuan Guan,[7] Melissa Goddard,[7] Erin Mitchell,[7] Jane Barber,[7] J. Koudy Williams,[7] David L. Mack,[1] Mark E. Furth,[8] Alban Vignaud,[3] Carole Masurier,[3] Fulvio Mavilio,[3] Philippe Moullier,[3,9,10] Alan H. Beggs,[5]* Anna Buj-Bello[3]*

Loss-of-function mutations in the myotubularin gene (*MTM1*) cause X-linked myotubular myopathy (XLMTM), a fatal, congenital pediatric disease that affects the entire skeletal musculature. Systemic administration of a single dose of a recombinant serotype 8 adeno-associated virus (AAV8) vector expressing murine myotubularin to *Mtm1*-deficient knockout mice at the onset or at late stages of the disease resulted in robust improvement in motor activity and contractile force, corrected muscle pathology, and prolonged survival throughout a 6-month study. Similarly, single-dose intravascular delivery of a canine AAV8-*MTM1* vector in XLMTM dogs markedly improved severe muscle weakness and respiratory impairment, and prolonged life span to more than 1 year in the absence of toxicity or a humoral or cell-mediated immune response. These results demonstrate the therapeutic efficacy of AAV-mediated gene therapy for myotubular myopathy in small- and large-animal models, and provide proof of concept for future clinical trials in XLMTM patients.

INTRODUCTION

Seminal clinical studies have recently shown that gene replacement therapy based on localized or systemic administration of adeno-associated viral (AAV) vectors has significant potential for the treatment of human monogenic diseases, such as retinal degeneration, metabolic disorders, or hemophilia (*1*–*4*). AAV vectors are excellent candidates to also treat neuromuscular diseases; however, to date, trials in patients with muscular dystrophies have been limited to local intramuscular injections with no obvious clinical benefit (*5*–*8*).

X-linked myotubular myopathy (XLMTM; OMIM 310400) is a fatal nondystrophic disease of skeletal muscle that affects about 1 in 50,000 male births. Patients typically present with marked hypotonia, generalized muscle weakness, and respiratory failure at birth (*9*). Survival beyond the postnatal period requires intensive support, often including gastrostomy feeding and mechanical ventilation. XLMTM results from loss-of-function mutations in the myotubularin 1 gene (*MTM1*) (*10*), which encodes the founder member of a family of 3-phosphoinositide phosphatases acting on the second messengers phosphatidylinositol 3-monophosphate [PI(3)P] and phosphatidylinositol 3,5-bisphosphate [PI(3,5)P_2] (*11*, *12*). Although myotubularin is expressed ubiquitously, loss of this enzyme primarily affects skeletal muscles. Myogenesis occurs, but muscle fibers throughout the body are hypotrophic and display structural abnormalities, with associated weakness (*13*). No effective therapy exists for XLMTM.

Animal models of the disease currently exist in zebrafish, mouse, and dog (*13*–*15*). Genetic disruption of *Mtm1* in mice causes profound abnormalities in skeletal muscle mass, structure, and function, regardless of whether expression is knocked out constitutively or only in a muscle-specific fashion (*13*, *16*). The murine phenotype resembles human XLMTM, with similar pathology and early mortality. Local injection of an *Mtm1* AAV vector rescued muscle function in the muscle-specific knockout (KO) model, indicating that restoration of functional myotubularin could ameliorate the disease phenotype (*17*). In the canine model—Labrador Retrievers carrying an X-linked *MTM1* missense mutation—muscles from affected males exhibit strongly reduced synthesis and altered localization of myotubularin, likely due to sequestration and degradation of the misfolded protein. The clinical picture closely resembles that of patients with comparably severe mutations, and survival does not normally exceed 4 months (*15*).

Here, we report the long-term therapeutic potential of systemic administration of an AAV8 vector expressing the myotubularin gene under the control of a muscle-specific promoter in the murine and canine models of XLMTM. In *Mtm1*-deficient mice, tail vein injection of AAV8-*Mtm1* at a dose of 10^{13} vector genomes per kilogram (vg/kg) at onset or at later stages of the disease corrected muscle pathology and prolonged survival throughout the 6-month study. In 9-week-old *MTM1*-deficient dogs, intravascular administration of AAV8-*MTM1* at the same dose was well tolerated, rescued the skeletal muscle pathology and respiratory function, and prolonged life for more than 1 year.

RESULTS

Systemic *Mtm1* delivery prolongs survival of *Mtm1*-deficient mice

Myotubularin KO mice (*Mtm1* KO) display muscle pathology by 3 weeks of age (fig. S1) and survive on average less than 2 months, as previously

[1]Department of Rehabilitation Medicine, School of Medicine, University of Washington, Campus Box 358056, Seattle, WA 98109, USA. [2]Institute for Stem Cell and Regenerative Medicine, University of Washington, Seattle, WA 98109, USA. [3]Généthon, 1 bis rue de l'Internationale, 91002 Evry, France. [4]Department of Human Nutrition, Foods and Exercise, Virginia Polytechnic Institute and State University, Blacksburg, VA 24061, USA. [5]Division of Genetics and Genomics, The Manton Center for Orphan Disease Research, Boston Children's Hospital, Harvard Medical School, 300 Longwood Avenue, Boston, MA 02115, USA. [6]Department of Pathology and Laboratory Medicine, Children's Hospital and Medical College of Wisconsin, Milwaukee, WI 53226, USA. [7]Wake Forest Institute for Regenerative Medicine, 391 Technology Way, Winston-Salem, NC 27101, USA. [8]Comprehensive Cancer Center, Wake Forest University Health Sciences, School of Medicine, Medical Center Boulevard, Winston-Salem, NC 27157, USA. [9]INSERM U649, Atlantic Gene Therapies, CHU Hôtel Dieu, 44300 Nantes, France. [10]Molecular Genetics and Microbiology Department, University of Florida, Gainesville, FL 32611, USA.
*Corresponding author. E-mail: abujbello@genethon.fr (A.B.-B.); beggs@enders.tch.harvard.edu (A.H.B.); mkc8@uw.edu (M.K.C.)

described (*13*, *18*). To correct the MTM1 deficiency, we developed a muscle-tropic serotype 8 AAV vector expressing the *Mtm1* complementary DNA (cDNA) under the control of a muscle-specific desmin promoter (AAV2/8-pDesmin-*Mtm1*, abbreviated AAV8-*Mtm1*). The vector was produced in human embryonic kidney (HEK) 293 cells by a tritransfection-based system, formulated for in vivo injection, and used to treat two groups of KO mice at different stages of disease evolution, at the early onset of the pathology (3 weeks of age) or at the late stage of the disease when mortality occurs (5 weeks of age) (Fig. 1A). A single tail vein injection of AAV8-*Mtm1* at a dose of 3×10^{13} vg/kg in *Mtm1* KO mice at 3 weeks (KO Early; $n = 8$) conferred long-term survival and nearly normal growth on 100% of the treated animals (Fig. 1B and movie S1). The same dose was administered to severely affected mice at 5 weeks (KO Late; $n = 11$), when 20% of the animals had already died. All treated mice remained viable and gained body mass over a 6-month observation period, except for a single 5-week-old mouse that died 1 day after injection (Fig. 1, B and C). Consistent with their robust appearance, skeletal muscles grew to normal size in vector-injected *Mtm1* KO mice. In both the early- and late-treated cohorts, each of the seven individual muscles analyzed gained mass, reaching >70% of the mass of wild-type muscle at 6 months (Fig. 1D).

Analysis of myotubularin expression by Western blotting in individual muscles at sacrifice demonstrated that intravenous delivery of AAV8-*Mtm1* reconstituted efficient myotubularin synthesis in skeletal muscles throughout the body. Myotubularin levels ranged between one- and fivefold greater than wild-type values in most skeletal muscles. There was no major difference between the early and late treatment cohorts, except for two peaks of >15-fold expression in the soleus muscle of early-treated KO mice and >40-fold expression in the tibialis anterior of late-treated KO mice (Fig. 1E). Myotubularin was highly overexpressed in the heart (720 ± 153 times the endogenous level 6 months after treatment) (fig. S2C). The AAV8-*Mtm1* average vector copy number (VCN; corresponding to viral genomes per diploid genome) in early- and late-treated mice was 0.72 ± 0.1 and 0.87 ± 0.1 in the tibialis anterior muscle and 1.67 ± 0.4 and 3.33 ± 2.1 in the biceps brachii muscle, respectively. VCN in the heart and liver ranged between 1.17 to 5.14 and 80 to 223 viral genomes/diploid genome, respectively, consistent with the known tropism of AAV8. At necropsy, the heart of AAV-treated KO mice showed the presence of some focal lesions with scar tissue and a modest cellular infiltrate, although these lesions did not affect survival in any of the treated *Mtm1* KO animals.

Mtm1 gene therapy corrects muscle pathology and function in myotubularin-deficient mice

The muscles of *Mtm1* KO mice treated with AAV8-*Mtm1* underwent sustained amelioration of pathological features. Figure 2 shows representative histology from the tibialis anterior and biceps brachii limb muscles of untreated, 5-week-old *Mtm1* KO mice and AAV-treated, 6-month-old KO mice, demonstrating normalized cross-sectional fiber size and intracellular architecture, as revealed by hematoxylin and eosin (H&E) and NADH (reduced form of nicotinamide adenine dinucleotide)–tetrazolium reductase (NADH-TR) staining (see fig. S2 for additional information). Morphometry of tibialis anterior and biceps brachii myofibers from 5-week-old *Mtm1* KO mice gave a mean diameter of 15.9 ± 0.8 μm and 17 ± 0.7 μm, respectively, with many fibers below 20 μm, compared to 28.7 ± 0.8 μm and 24.3 ± 1.2 μm for wild-type mice (Fig. 2B and fig. S2A). Six months after treatment with AAV8-*Mtm1*, the abundance of extremely small-diameter myofibers was eliminated, and the size distribution approached that of wild-type muscles in both cohorts. In addition, myofibers of treated mice displayed a reduced frequency of centrally localized nuclei, a diagnostic feature of centronuclear myopathies like XLMTM (fig. S2B).

Distinctive features of myotubularin-deficient myofibers include aberrant accumulations of mitochondria (*13*) and a marked deficiency of transverse tubules (T-tubules), invaginations of the plasma membrane perpendicular to the length of the myofiber that are critical for excitation-contraction coupling and muscle function (*14*, *18*). Untreated *Mtm1* KO mice showed abnormal localization of proteins associated with the T-tubule system, including the dihydropyridine 1α receptor (DHPR1α), a voltage-gated Ca^{2+} channel, and dysferlin, a transmembrane protein involved in Ca^{2+}-dependent membrane repair (Fig. 2A, arrows). Treatment with AAV8-*Mtm1* corrected abnormal mitochondria distribution and cellular mislocalization of DHPR1α and dysferlin in all mice from both early- and late-treated cohorts, indicating that XLMTM-associated pathology can be reversed well after the onset of the disease.

Structural muscle abnormalities are mirrored by severe functional deficits in *Mtm1* KO mice. To measure the effect of gene therapy on muscle function, we used the open-field actimeter, global muscle strength, and isolated limb strength assays. Open-field actimeter measurements showed that mutant mice covered less than half the distance explored by wild-type mice at 5 weeks of age (Fig. 3A). Mice treated with AAV8-*Mtm1* at both early and late stages of the disease showed significant functional improvement, and at 6 months after AAV injection, their motor activity was indistinguishable from that of wild-type animals. A noninvasive test of global muscle strength that measures forward pulling tension in an escape paradigm revealed that untreated *Mtm1*-deficient mice were half as strong as wild-type mice (whole-body tension, 0.07 ± 0.01 versus 0.15 ± 0.01 N/g; $P < 0.01$) (Fig. 3B). Early- and late-treated mice showed 82% (0.15 ± 0.01 N/g) and 76% (0.13 ± 0.01 N/g) recovery of whole-body tension, respectively (Fig. 3B). In a functional assay of an isolated hindlimb muscle, the extensor digitorum longus, the isometric force of untreated *Mtm1* KO mice was only 13% of the wild-type level, whereas it almost normalized 6 months after AAV8-*Mtm1* delivery in both cohorts ($P = 0.0016$ and $P < 0.001$ for the early- and late-treated groups of mice, respectively; Fig. 3C). Together, these data indicate that muscle impairment associated with myotubularin deficiency can be rescued by gene therapy even after the onset of pathology.

Correction of muscle pathology in myotubularin-deficient mice is dose-dependent

To assess the effect of a lower vector dose on phenotype correction, we injected AAV8-*Mtm1* (5×10^{12} vg/kg) into the tail vein of *Mtm1* KO mice at 3 weeks of age ($n = 10$). This dose prolonged the survival of 50% of the mice over 3 months, with the first death occurring 6 weeks after injection (fig. S3A). Body weight increased during the first 3 weeks of treatment and remained unchanged after this period (fig. S3B). This partial recovery of body mass was reflected at the level of individual skeletal muscles: two of the seven analyzed muscles (soleus and biceps brachii) grew normally, whereas the other five reached 40 to 60% of wild-type mass at 3 months (fig. S3C). The motor activity of mice treated with the low vector dose appeared indistinguishable from that of wild-type mice and KO mice treated with the high dose in an open-field actimeter assay 3 months after injection (fig. S3E). However, their global muscle strength was reduced by 55% in the more sensitive escape test, and their isolated soleus and extensor digitorum longus muscles gener-

ated 60 and 9% of the wild-type force, respectively, indicating that muscle function recovery was not complete in the low-dose cohort. In the extensor digitorum longus muscle, only 3% of the myotubularin endogenous level was reached (fig. S3D), ranging from 7 to 27% in the other analyzed muscles (mean = 13%), indicating that low levels of MTM1 are sufficient to prolong the survival of mutant mice.

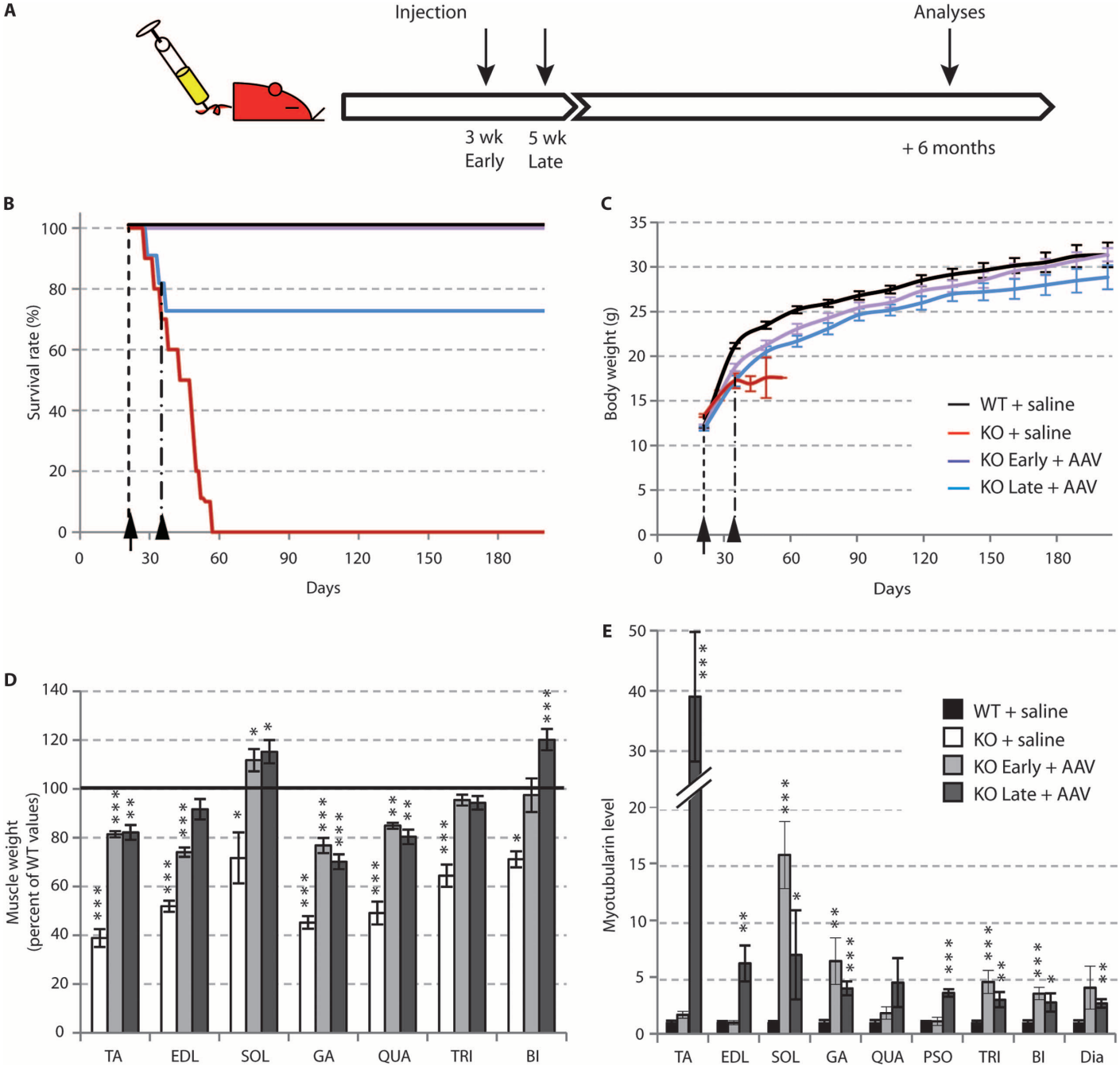

Fig. 1. Intravascular delivery of AAV8-*Mtm1* in myotubularin-deficient mice improves life span and body growth. (**A**) Experimental design. (**B** and **C**) Survival (B) and body mass (C) of wild-type (WT) mice and constitutive KO-*Mtm1* mice injected at 3 weeks of age with saline (WT + saline, KO + saline, $n = 10$ per genotype). Myotubularin-deficient mice were injected with AAV8-*Mtm1* at 3×10^{13} vg/kg at 3 (KO Early + AAV, $n = 8$) and 5 weeks of age (KO Late + AAV, $n = 11$) in a 6-month study. (**D**) Mass of representative skeletal muscles of KO-*Mtm1* mice 2 weeks after injection of saline (KO + saline, $n = 4$) and 6 months ($n = 10$) after injection of AAV8-*Mtm1* (KO Early + AAV, $n = 8$; KO Late + AAV, $n = 8$). Values were normalized to muscle mass of age-matched, saline-injected WT mice ($n = 10$), taken as 100%. (**E**) Myotubularin protein quantification by immunoblot; glyceraldehyde-3-phosphate dehydrogenase (GAPDH) immunodetection was used as an internal control. The number of animals was as in (C). Muscles: TA, tibialis anterior; EDL, extensor digitorum longus; SOL, soleus; GA, gastrocnemius; QUA, quadriceps; TRI, triceps; BI, biceps brachii; DIA, diaphragm. $^{*}P < 0.05$; $^{**}P < 0.01$; $^{***}P < 0.001$, Mann-Whitney test, each condition versus WT + saline values.

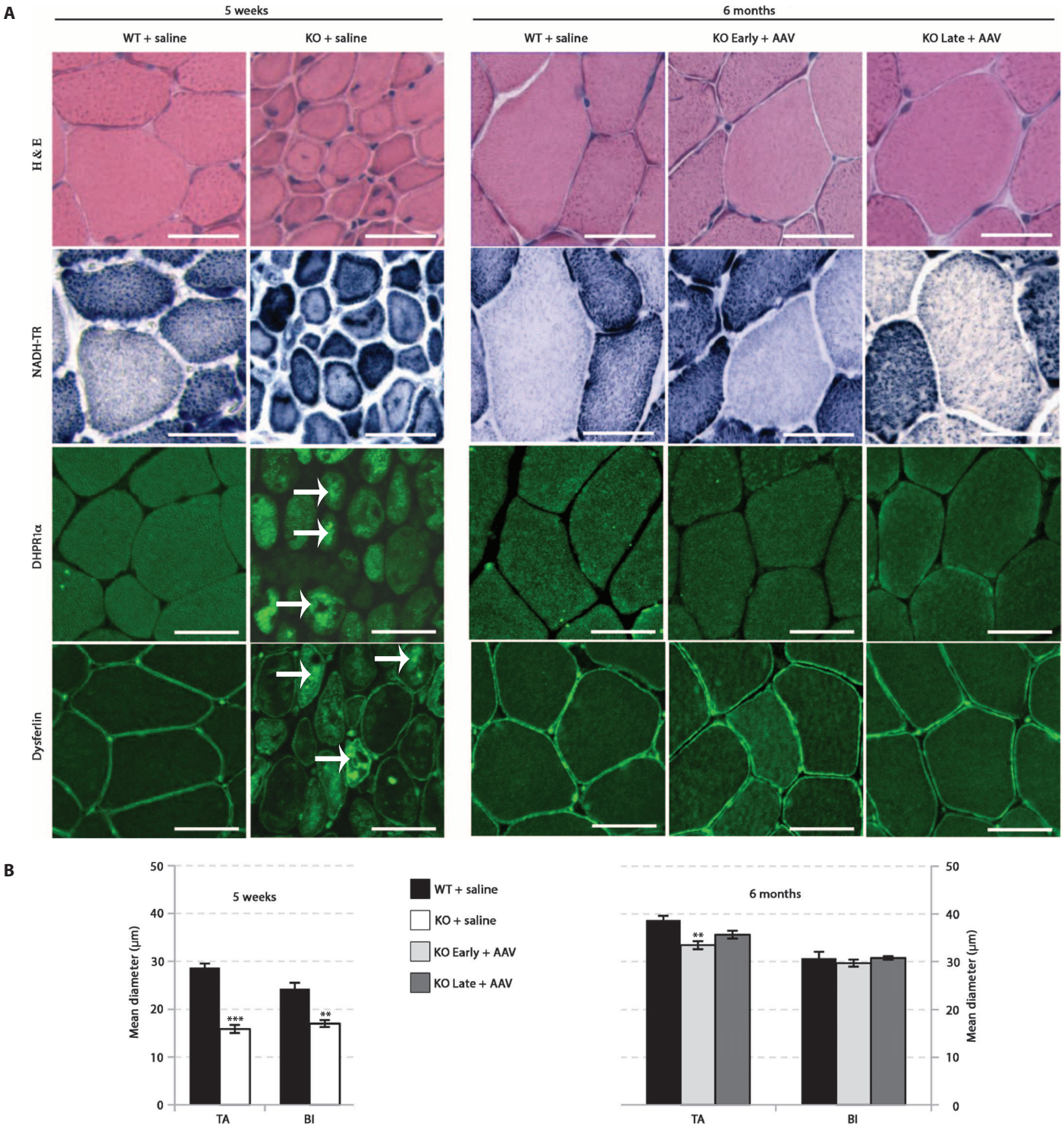

Fig. 2. *Mtm1* gene therapy corrects the internal architecture and hypotrophy of skeletal muscle fibers in myotubularin-deficient mice. Treatment groups were as described in Fig. 1. Myotubularin-deficient mice were injected with AAV8-*Mtm1* at 3×10^{13} vg/kg at 3 (KO Early + AAV, $n = 8$) and 5 weeks of age (KO Late + AAV, $n = 11$) in a 6-month study. Mice were injected with either saline (+ saline) or AAV8-*Mtm1* vector (+ AAV). Sections were obtained after 2 weeks (5 weeks of age) and after 6 months of treatment. (**A**) Cross sections from tibialis anterior (TA) muscle stained with H&E and NADH-TR and by immunofluorescence with antibodies against DHPR1α and dysferlin. White arrows indicate abnormal localization of proteins. Scale bars, 10 μm. (**B**) Mean diameter of muscle fibers from tibialis anterior and biceps brachii muscles from mice injected with either saline or AAV8-*Mtm1* after 2 weeks (left graph; WT + saline, $n = 10$; KO + saline, $n = 4$) and after 6 months of treatment (right graph; WT + saline, $n = 10$; KO Early + AAV, $n = 7$; and KO Late + AAV, $n = 8$). $^{**}P < 0.01$; $^{***}P < 0.001$, *t* test, each condition versus WT + saline values.

Intramuscular injection of AAV8-*MTM1* ameliorates pathology and increases strength of myotubularin-deficient canine muscles

To evaluate myotubularin gene replacement therapy in a large-animal model, we studied male XLMTM Labrador/Beagle F1 offspring, which display the same pathology and clinical features as the previously reported XLMTM pure-bred Labradors (*15*). These dogs become symptomatic by 9 to 10 weeks of age, and muscular weakness progresses up to ~18 weeks of age, when animals can no longer ambulate and rapidly die. For this study, we generated a recombinant AAV8 vector carrying the canine *MTM1* cDNA under the control of the desmin promoter as in the murine vector (AAV2/8-pDesmin-*MTM1* or AAV8-*MTM1*). The vector was produced in Sf9 cells by a baculovirus-based system, purified by affinity chromatography, and formulated for in vivo injection. To assess transgene expression and the local effect on diseased muscle, we injected a single dose of 4×10^{11} vg of the AAV8-*MTM1* vector into the middle part of the cranial tibialis hindlimb muscle of XLMTM dogs at 10 weeks of age ($n = 3$). The contralateral muscles received only saline. Dogs were sacrificed after 4 to 6 weeks, and injected muscles were analyzed for histological appearance, protein expression, and function. All AAV-treated muscles grew in mass and volume by about 50% compared to the contralateral, saline-injected muscles, as shown by weight/volume measurements and computed tomography scans (Fig. 4A and fig. S4). AAV-injected muscles consistently showed improved architecture, with increased myofiber size, normalization of mitochondria positioning, and cellular localization of DHPR1α and dysferlin (Fig. 4C). Electron microscopy confirmed that, compared to wild-type muscle, XLMTM muscle contained few characteristic T-tubules but showed atypical longitudinal structures (L-tubules). By contrast, AAV8-*MTM1*–injected mutant muscles closely resembled wild type, with abundant T-tubules (Fig. 4C and table S1). Expression of vector-driven MTM1 protein was analyzed on whole-muscle lysates by Western blotting with an antibody against canine myotubularin. Immunoblot analysis showed substantial myotubularin expression in the injected muscles of all treated dogs (Fig. 4A), decreasing from about 60% of the wild-type levels at the center of the cranial tibialis to about 8% at its ends. Some myotubularin expression was detected in the contiguous extensor digitorum longus muscles, whereas no expression was detected in the contralateral limb muscles or in distant muscles such as the diaphragm or the heart.

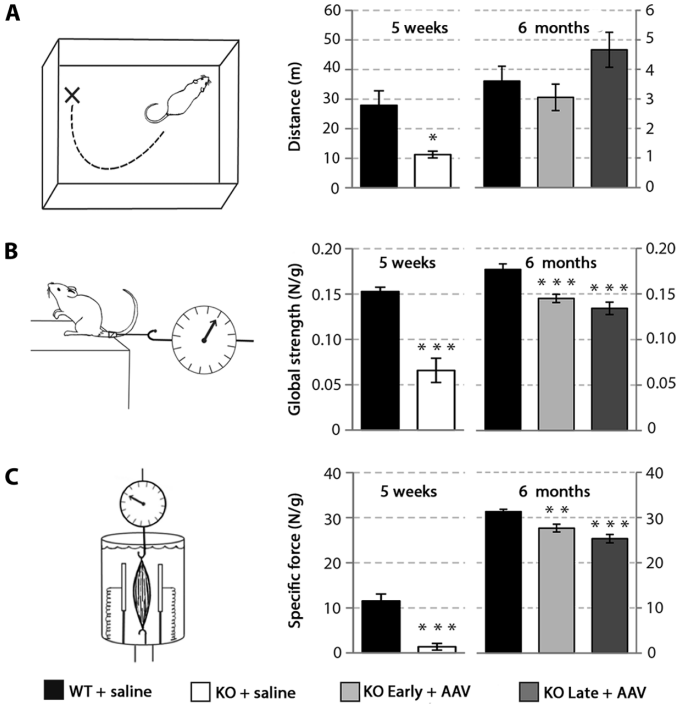

Fig. 3. Gene therapy with AAV8-*Mtm1* improves strength, activity, and long-term survival in myotubularin-deficient mice. (**A**) Whole-body spontaneous mobility of normal (WT + saline), mutant (KO + saline), and AAV-treated mutant (KO Early + AAV and KO Late + AAV) mice 2 weeks (5 weeks of age) and 6 months after phosphate-buffered saline (PBS) or vector injection. The distance covered over the 90-min test was assessed with an open-field actimeter. (**B**) Escape test measurements in the same five groups of mice (WT + saline and KO + saline at 5 weeks; WT + saline, KO Early + AAV, and KO Late + AAV at 6 months). (**C**) Specific tetanic force of isolated extensor digitorum longus muscles from KO mice injected at an early and late stage of the disease 6 months after vector delivery compared to saline-injected KO and WT littermates. WT + saline ($n = 6$) and KO + saline ($n = 4$) at 5 weeks; WT + saline ($n = 10$), KO Early + AAV ($n = 8$), and KO Late + AAV ($n = 8$) at 6 months. *$P < 0.05$; **$P < 0.01$; ***$P < 0.001$, *t* test.

To evaluate the effect of treatment on muscle function, we used force transduction assays developed to assess the strength of the distal part of canine hindlimbs during flexion, mainly generated by the cranial tibialis muscle (Fig. 4B depicts an isometric contraction assay) (*19*–*21*). Immediately before gene therapy at 10 weeks of age (baseline), XLMTM dogs were slightly weaker than unaffected wild-type littermates, and the two hindlimbs of each dog performed equally (Fig. 4B). Measurements of force 4 and 6 weeks later showed more than doubled limb strength in wild-type dogs, consistent with normal muscular maturation. In mutant dogs, the strength of AAV8-*MTM1*–treated limbs increased strikingly only 4 weeks after injection and reached 80% of wild-type force at 6 weeks, whereas limbs injected with saline did not improve. We also used a dynamic eccentric contraction assay to measure muscular performance over prolonged exercise (fig. S5). When assessed by this test, the hindlimbs of young wild-type dogs strengthened over time, whereas saline-injected limbs of all three XLMTM dogs declined to about 20% of wild-type values. Again, injection of AAV8-*MTM1* greatly improved muscle performance: at 14 and 16 weeks of age, treated limbs achieved >70% of wild-type strength (fig. S5, B to D). These results showed that a single injection of AAV8-*MTM1* is efficacious in rescuing the function of an entire myotubularin-deficient muscle, prompting us to assess an intravascular delivery approach.

Intravascular administration of AAV8-*MTM1* rescues muscle pathology and prolongs survival of XLMTM dogs

AAV delivery by isolated limb perfusion allows widespread transduction of muscle groups in dogs and nonhuman primates (*22*–*24*). To test whether regional administration is sufficient to ameliorate muscle pathology in an entire limb, we injected a single dose of AAV8-*MTM1* (2.5×10^{13} vg/kg) under high pressure into the saphenous vein of three 9-week-old XLMTM dogs, after applying a tourniquet around the hindlimb distal to the injection site to limit blood circulation during infusion. The tourniquet was released 5 min after injection. Treated dogs improved in strength rapidly after vector administration. In contrast to dogs injected intramuscularly, where only the muscles of the injected limb gained strength, high-pressure intravascular limb delivery of AAV8-*MTM1* resulted in improved strength of both the infused and contralateral hindlimbs, which

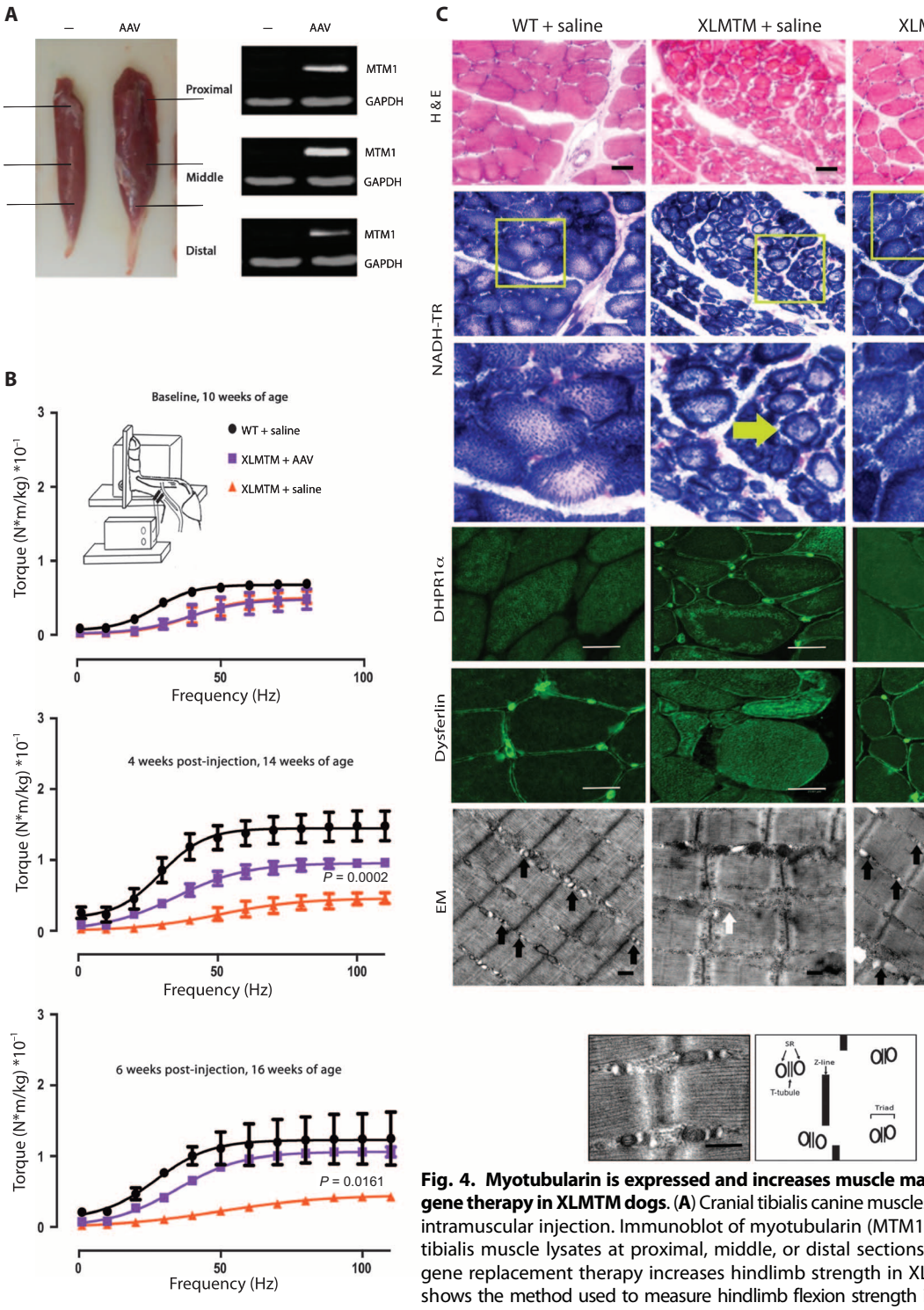

Fig. 4. Myotubularin is expressed and increases muscle mass and volume after local gene therapy in XLMTM dogs. (**A**) Cranial tibialis canine muscles 6 weeks after AAV8-*MTM1* intramuscular injection. Immunoblot of myotubularin (MTM1) and GAPDH from cranial tibialis muscle lysates at proximal, middle, or distal sections of the muscle. (**B**) MTM1 gene replacement therapy increases hindlimb strength in XLMTM dogs. The drawing shows the method used to measure hindlimb flexion strength in dogs. A nerve stimulator delivers electrical frequencies from 1 to 110 Hz to muscles that pull the paw toward the stifle (knee). A transducer captures the torque generated when the paw pulls on the foot pedal. Upper graph: baseline before injection, 10 weeks of age (WT, $n = 3$; XLMTM, $n = 3$); middle graph: 4 weeks after injection, 14 weeks of age (WT, $n = 3$; XLMTM, $n = 3$); bottom graph: 6 weeks after injection, 16 weeks of age (WT, $n = 2$; XLMTM, $n = 2$). $P = 0.002$ (4 weeks after injection); $P = 0.0161$ (6 weeks after injection; XLMTM + AAV versus WT + saline values), one-way analysis of variance (ANOVA). (**C**) Local myotubularin gene replacement therapy improves muscle fiber architecture in XLMTM dogs. Cryosections of the cranial tibialis muscle (middle part) were assessed microscopically: boxes in NADH-TR staining show areas magnified below; immunofluorescence staining for DHPR1α and dysferlin shows correction of abnormal organelles with AAV8-*MTM1* (yellow arrow). Scale bars, 25 μm. Electron microscopy (EM) shows normal T-tubules (black arrows) and abnormal L-tubules (white arrow). Scale bar, 500 nm. Bottom panel: Close-up of WT muscle and schematic showing normal relationship of sarcomere ends (Z-line), and triads of T-tubules and sarcoplasmic reticulum (SR).

reached on average almost normal values 6 weeks after infusion (Fig. 5A and fig. S6). Similarly, peak inspiratory flow (PIF) (the fastest flow rate measured during inhalation) was strongly reduced in XLMTM dogs at 16 weeks of age, but was normal in treated dogs (Fig. 5B), indicating that the AAV8-*MTM1* vector transduced respiratory muscles and improved their function. Most importantly, all treated dogs showed a marked improvement in survival, which extended far beyond the critical 18-week time point, when all untreated XLMTM dogs could no longer ambulate and needed to be euthanized. The first infused XLMTM dog (dog 4) survived in relatively good condition beyond 1 year and was sacrificed for analysis at 14 months of age. The other two dogs (dogs 5 and 6) remained ambulant and clinically robust beyond the age of 1 year, and were alive and healthy at the time of manuscript preparation (movie S2).

Muscle biopsies were taken from the injected and contralateral hindlimbs (quadriceps and biceps femoris) and from the forelimbs (triceps and biceps brachii) of all treated dogs 4 weeks after infusion to analyze vector distribution, transgene expression, and histology. Intravenous administration of AAV8-*MTM1* improved myofiber appearance and architecture in the treated limbs, which consistently showed an average fiber size only slightly reduced compared to wild-type muscles measured 4 weeks after infusion (Fig. 6A). In contrast, at 1 year after infusion, noninfused limbs displayed heterogeneity in muscle fiber size, with coexistence of small and large fibers (Fig. 6B). Electron microscopy performed on quadriceps muscle samples obtained from all infused limbs showed normalized sarcotubular organization, similar to what was observed after intramuscular injection (table S2). The biceps femoris muscles of dog 4, analyzed at sacrifice, revealed a partially defective sarcotubular organization in both the infused and noninfused hindlimb, with only about one triad per field in each muscle (table S3).

Real-time polymerase chain reaction (PCR) and Western blot analysis demonstrated both AAV8 vector (Fig. 7A) and myotubularin (Fig. 7B and fig. S7) expression in all muscle samples obtained from all three treated dogs: 4 weeks after infusions, the level of myotubularin expression reached 21 to 72% of the wild-type control levels in the biceps femoris and quadriceps muscles in the injected limbs and 9 to 138% in the muscles (quadriceps, biceps femoris, triceps, and biceps brachii) of the noninjected limbs. Expression levels were paralleled by VCN levels, which ranged from 0.52 to 2.35 in the biceps femoris and quadriceps muscles of the infused limbs and from 0.17 to 3.65 in the muscles of the noninjected limbs (Fig. 7A). The biodistribution of AAV8-*MTM1* was analyzed in dog 4 at necropsy. The VCN was, in general, higher in infused muscles (range, 0.01 to 2.27) than in distal muscles (range, 0.007 to 0.13; $n = 18$), with the exception of the diaphragm, intercostal muscles, and heart, where we detected a VCN of 0.37, 0.59, and 0.28, respectively (Fig. 7C). MTM1 protein levels were above the endogenous level in 7 of 13 muscles from the infused hindlimb and barely detectable in the contralateral and forelimb muscles (Fig. 7D), mirroring the VCN values and suggesting that very low amounts of myotubularin are sufficient to rescue muscle function. In the diaphragm and heart, myotubularin reached 64 and 13% of the wild-type values, respectively. The heart of dog 4 showed no signs of toxicity at histological examination (fig. S8) and at the functional level, as assessed by electrocardiogram and echocardiography before necropsy. The histology of the liver (VCN: 0.63) was also normal, and myotubularin protein was undetectable.

These data show that isolated limb perfusion was effective in delivering the AAV vector to the infused muscle groups but did not limit vector diffusion to other organs, including the rest of the skeletal musculature and the heart.

Intramuscular or intravascular delivery of AAV8-*MTM1* elicits no humoral or cytotoxic immune response against the transgene product in XLMTM dogs

The neutralizing factor (NAF), immunoglobulin G (IgG), and IgM titers specific to AAV8 were measured in XLMTM dog sera before and after intramuscular (fig. S9A) or intravascular (fig. S9B) administration of AAV8-*MTM1*. NAF and IgG titers increased 1 week after injection and remained elevated for up to 10 months in all treated animals, whereas IgM titers decreased to preinfusion levels in dogs treated by intravascular infusion. Conversely, MTM1-specific IgG or IgM antibodies remained undetectable in all treated animals (fig. S9, C and D). Cell-mediated immune responses against the vector or the transgene product were tested by an interferon-γ (IFN-γ) enzyme-linked immunospot assay on peripheral blood mononuclear cells over a period of 155 days after vector administration. We were unable to detect any T cells specific to the vector capsid or the MTM1 protein in XLMTM dogs given intramuscular or intravenous AAV8-*MTM1* (fig. S10).

Inflammatory cytokines [interleukin-2 (IL-2), IL-6, IL-8, IL-10, IL-15, tumor necrosis factor–α (TNF-α), and IFN-γ] were profiled in XLMTM dogs before and after intramuscular or intravascular infusion of AAV8-*MTM1* (table S4). Of the three dogs injected intramuscularly, one (dog 3) displayed elevated TNF-α levels (42.5 to 80.8 pg/ml) between day 3 and day 28 after injection. Transient elevation of IL-2 and IL-15 levels (743.5 and 119 pg/ml, respectively) was observed in only one dog treated intravascularly (dog 6) 6 hours after infusion. No elevation of inflammatory cytokines levels was observed in the other animals, including untreated controls, throughout the observation period.

DISCUSSION

Gene therapy of neuromuscular disorders requires body-wide distribution of the therapeutic gene and, therefore, systemic delivery of a gene transfer vector capable of transducing skeletal muscles and, if necessary, the heart. AAV vectors are attractive candidates because of their natural tropism for muscle and their small size, which allows access to fibers through the vascular endothelium and the basement membrane. Preclinical and clinical studies proved that AAV-mediated delivery can lead to transgene expression at therapeutic or subtherapeutic levels in entire muscles and can correct the disease phenotype in animal models of muscular dystrophy [reviewed in (*25*)]. Clinical trials showed, however, that intramuscular injection is impractical and unlikely to provide significant clinical benefit to patients affected by limb girdle or Duchenne muscular dystrophy (DMD) (*5*–*8*). Initial efforts aimed at targeting skeletal and cardiac muscles through intravascular delivery required the use of invasive procedures and relatively toxic permeabilizing drugs (*26*). However, the introduction of muscle-tropic serotypes such as AAV6, AAV8, and AAV9 allowed the transduction of both skeletal and cardiac muscle by low-pressure intravascular or systemic intravenous administration, and achieved significant phenotypic correction in both murine and canine models of muscular dystrophy (*27*–*30*). Systemic AAV administration has not yet been attempted in patients.

Here, we show long-term full phenotypic correction of MTM1-deficient myotubular myopathy in both a murine and a canine model of the disease by intravenous administration of an AAV8 vector carrying a muscle-specific MTM1 expression cassette. In mice, a single tail vein administration of the AAV8-*Mtm1* vector either before or after the onset of the pathology achieved full rescue of the disease for the duration of the

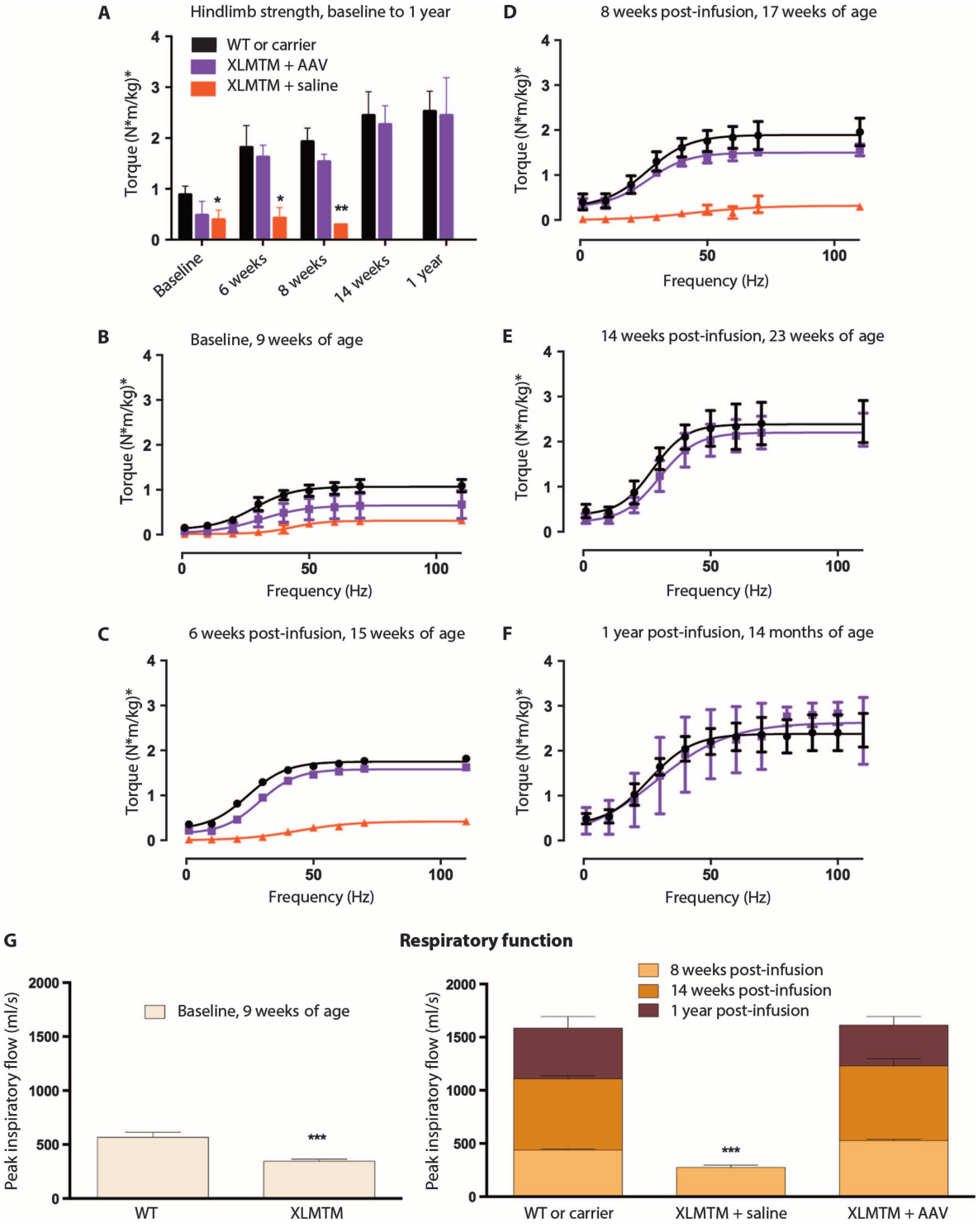

Fig. 5. Hindlimb strength of XLMTM dogs after intravascular administration of AAV8-*MTM1*. Data are presented as means ± SD combined values of both limbs. (**A**) Peak hindlimb torque at various times up to 1 year after infusion. (**B**) Baseline before infusion, 9 weeks of age (WT, n = 2; XLMTM + AAV8, n = 3; XLMTM + saline, n = 1). (**C**) Six weeks after infusion, 15 weeks of age (WT, n = 2; XLMTM + AAV8, n = 2; XLMTM + saline, n = 2). (**D**) Eight weeks after infusion, 17 weeks of age (WT, n = 3; XLMTM + AAV8, n = 3; XLMTM + saline, n = 3). (**E**) Fourteen weeks after infusion, 23 weeks of age (WT, n = 3; XLMTM + AAV8, n = 3). XLMTM dogs infused only with saline did not survive beyond 18 weeks of age. (**F**) One year after infusion (WT, n = 1; carrier, n = 3; XLMTM + AAV8, n = 3). (**G**) PIF, a respiratory functional measure reflecting diaphragm muscle strength, taken in anesthetized dogs at baseline and at 8 weeks, 14 weeks, and 1 year after infusion with AAV8. Number of animals per group was the same as in (B) to (F). ***P < 0.001, one-way ANOVA, each condition versus WT + saline values.

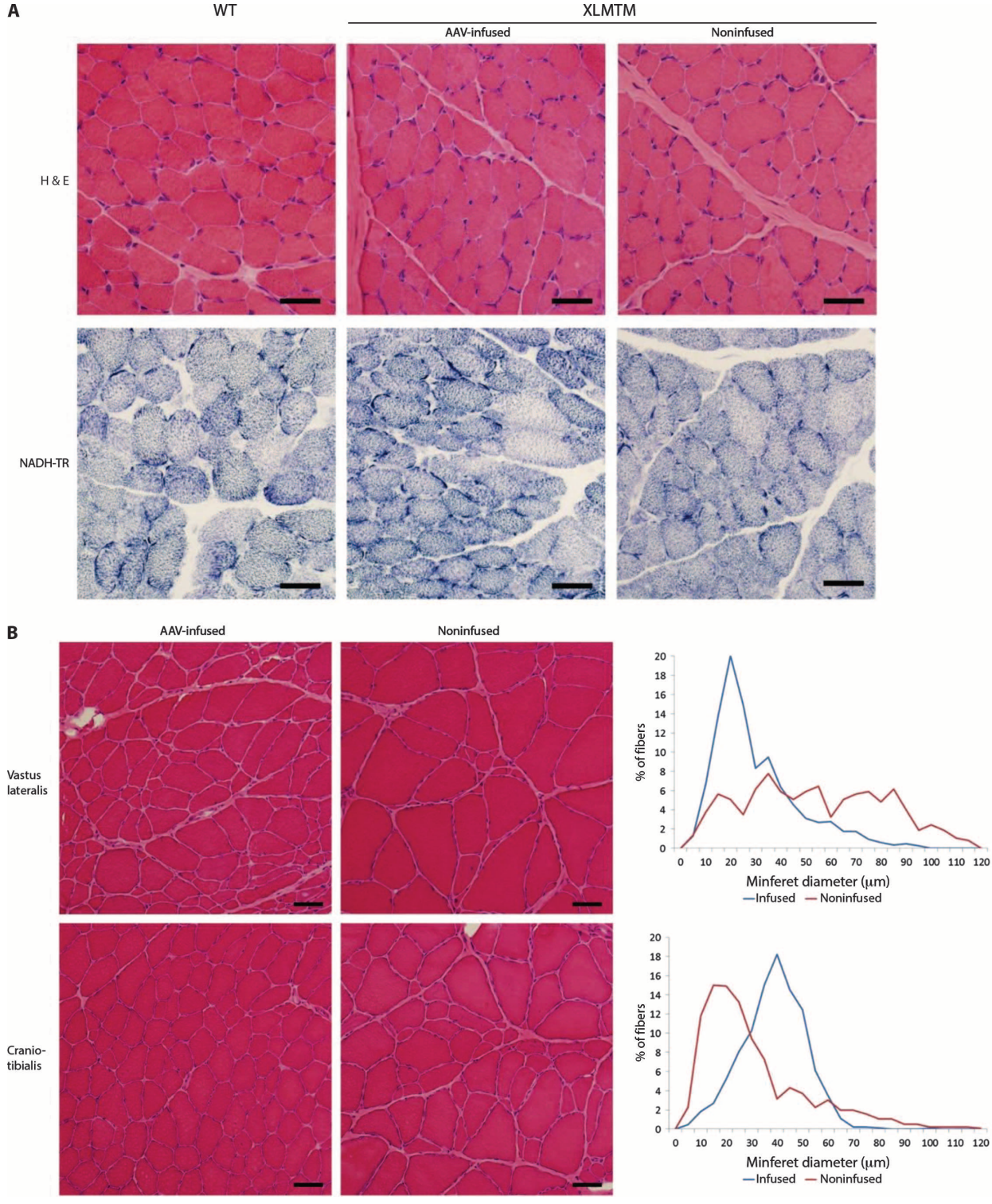

Fig. 6. *MTM1* gene therapy corrects the internal architecture and hypotrophy of skeletal muscle fibers in myotubularin-mutant dogs. Muscle cryosections from age-matched WT or AAV8-*MTM1*–infused XLMTM dogs were assessed microscopically. Comparison is shown between the left (infused) hindlimb and the right (contralateral noninfused) limb. (**A**) Representative micrographs of quadriceps muscle cross sections from muscle biopsies taken 4 weeks after infusion from dog 4 stained with H&E or NADH-TR. (**B**) H&E-stained cranial tibialis muscle cross sections taken 1 year after AAV infusion. Graphs indicate myofiber diameter frequency distribution of corresponding images for the vastus lateralis muscle (upper graph) and craniotibialis muscle (lower graph). Scale bars, 25 μm.

study. The fact that the MTM1 pathology could be corrected in already severely affected mice indicates that the damage induced by the absence of MTM1 is reversible, a particularly important finding in view of a clinical translation of XLMTM gene therapy, which will inevitably involve already symptomatic patients. However, differences exist between the clinical presentation of XLMTM in patients compared to animal models. In particular, patients typically present with respiratory failure at birth, whereas mice and dogs develop respiratory weakness later in life. Thus, it may be necessary to develop specific clinical protocols for treating very young children and balance the risk of treatment versus that of assisted ventilation.

To confirm the therapeutic potential of the AAV8-*MTM1* vector in the XLMTM dog model, we decided to use a clinically relevant delivery method based on isolated limb perfusion. This delivery route showed feasibility and safety in a clinical trial on volunteer patients affected by several forms of muscular dystrophy (*31*). We intended to use high-pressure intravascular hindlimb administration as an intermediate approach between direct intramuscular muscle injection, which confirmed the therapeutic potential of the AAV8-*MTM1* vector even in large muscles, and full systemic administration. Surprisingly, we observed a marked rescue of the lethality and a systemic correction of the skeletal muscle pathology in all treated dogs throughout the duration of the 1-year study. Intravascular delivery of the AAV8-*MTM1* vector under pressure against a tourniquet led to efficient transduction not only of all muscles in the infused limb but also of distal muscles and organs, although at a lower level in terms of both VCN and protein expression. The respiratory muscles, and particularly the diaphragm, were well transduced and their function was normalized in all animals. This is the first demonstration of complete and persistent phenotypic correction of a monogenic neuromuscular disease in a large-animal model by a single intravenous

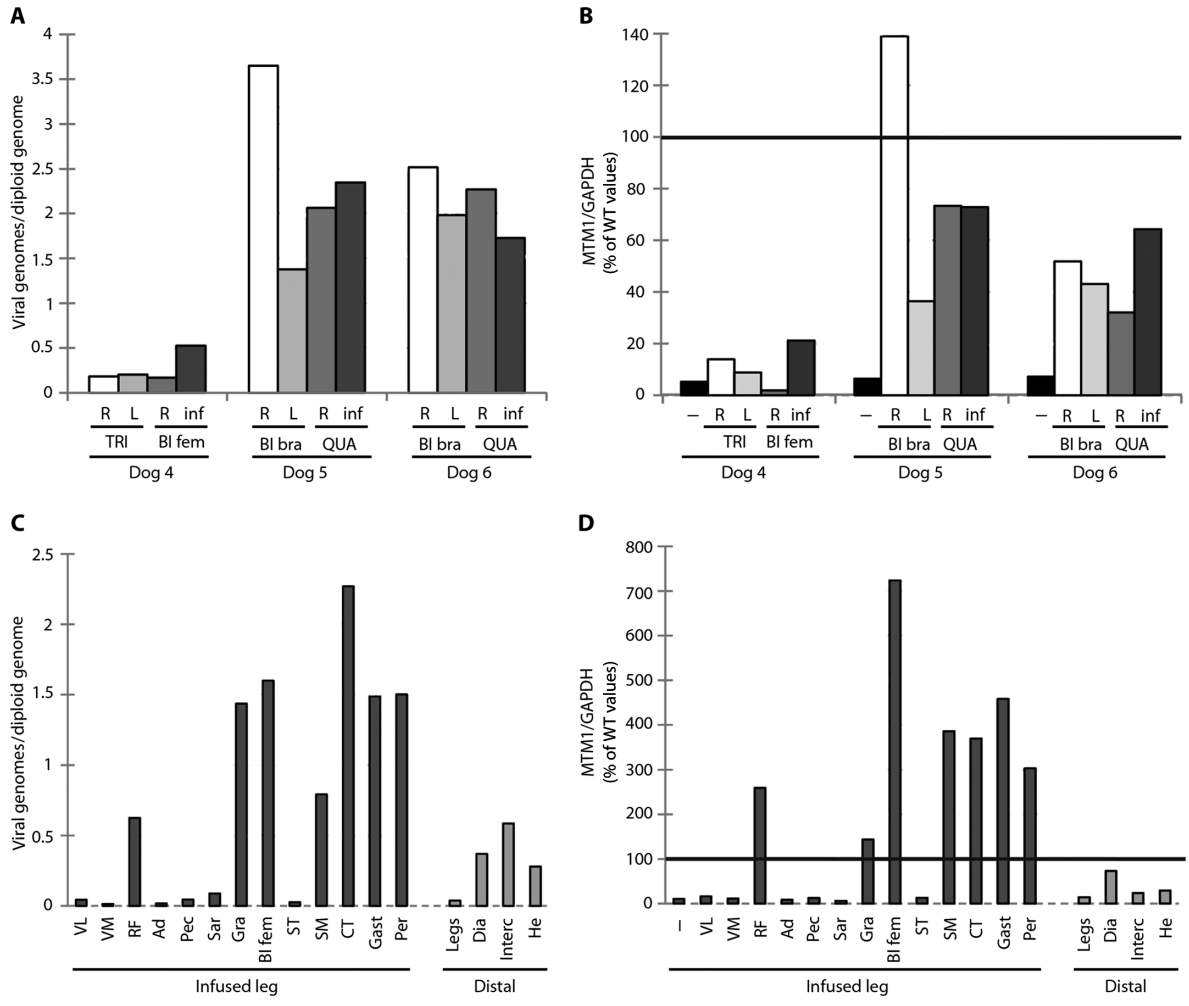

Fig. 7. Biodistribution of AAV8 vector and myotubularin transgene expression in XLMTM dogs infused with AAV8-*MTM1*. (**A** and **B**) Comparison of vector distribution (A) and MTM1 transgene expression (B) among upper and lower limb muscle biopsies collected 4 weeks after infusion in three XLMTM dogs: dogs 4 to 6. Upper limb muscles: triceps (TRI) and biceps brachii (Bl bra). Lower limb muscles: biceps femoris (Bl fem) and quadriceps (QUA). R, right; L, left; inf, infused limb. (B) Expression of canine MTM1 protein relative to the housekeeping gene GAPDH in whole-muscle lysates probed with an anti-myotubularin antibody. (**C** and **D**) Comparison of vector distribution (C) and MTM1 transgene expression (D) among upper and lower limb muscle necropsy samples collected 1 year after infusion in dog 4, an XLMTM dog. Muscles of the infused leg: VL, vastus lateralis; VM, vastus medialis; RF, rectus femoris; Ad, adductor magnus; Pec, pectineus; Sar, cranial sartorius; Gra, gracilis; Bl fem, biceps femoris; ST, semitendinosus; SM, semimembranosus; CT, cranial tibialis; Gast, gastrocnemius; Per, peroneus longus. Muscles distal to the infused leg: Dia, diaphragm; Interc, intercostals; He, heart.

administration of an AAV vector. Our results indicate that systemic intravenous administration may be the simplest and most effective way of administering an AAV-based gene therapy for XLMTM in patients, although additional dose-finding and toxicity studies will be necessary before launching a clinical trial.

The unpredicted systemic effect of the high-pressure intravascular vector administration in the present study is in contrast with previous studies of tightly restricted vector transduction in the limbs of hemophilic and golden retriever muscular dystrophy (GRMD) dogs, infused with AAV1 or AAV2 vectors (*24*, *32*). Although blood flow was monitored in the present study by ultrasound above and below the constriction during infusion, the tourniquet was apparently inefficient in limiting vector delivery to the infused limb because of slippage, collateral circulation, or other less obvious factors. The tourniquet was released after 5 min, when a substantial amount of vector was apparently still available to enter the systemic circulation and transduce distant organs. A longer persistence of the AAV8 with respect to an AAV1 or AAV2 vector in the isolated limb circulation might have also contributed to the ineffective restriction. The gradient of VCN distribution above and below the tourniquet was more pronounced in the first treated dog, dog 4, than in the subsequent two, dogs 5 and 6, where the vector transduced almost uniformly all muscles, indicating a certain variability in the limb isolation procedure.

The quasi-systemic vector administration was well tolerated by all three XLMTM dogs, which showed no signs of acute or chronic toxicity. Liver enzyme levels were within the normal range in all dogs throughout the study, and the histology of dog 4's liver appeared to be normal at necropsy. Likewise, no toxicity was observed in the systemically treated mutant mice, with the exception of focal heart inflammatory infiltrates and fibrotic lesions detected in animals treated at the highest dose (3×10^{13} vg/kg), but otherwise asymptomatic. This was not observed in the heart of dog 4 at necropsy, which was completely normal 1 year after vector administration. The desmin promoter is very active in cardiac muscle (*33*) and caused a marked MTM1 overexpression in murine heart. Conversely, MTM1 expression was below the endogenous level in the heart of dog 4, which was treated with a similarly high dose compared to the mouse study (2.5×10^{13} vg/kg), although through a different route. This suggests that accessibility from the systemic circulation, heart tropism of the AAV8 vector, or desmin promoter function may vary among different species, and indicates the need for a specific toxicity study in large animals before advancing to a clinical trial.

Our study shows that the threshold of myotubularin expression required for therapeutic benefit in XLMTM mice and dogs is well below the normal levels and may vary among different muscles, as observed for other neuromuscular disorders because of enzyme rather than structural protein deficiency (*34*). In *Mtm1* KO mice, administration of low levels of an engineered myotubularin protein was sufficient to improve both muscle function and pathology (*35*). In other studies, mice carrying an engineered *Mtm1* missense mutation that affects RNA splicing and leaves just traces of myotubularin activity survive eight times longer than constitutive *Mtm1* KO mutants (*36*). Here, the amount of myotubularin present in skeletal muscles of mice 6 months after high-dose vector injection ranged between one and five times the endogenous levels, leading to full correction. A lower vector dose led to synthesis of 3 to 27% of the normal myotubularin levels in treated mice, which was curative for some but not all muscles but was still able to prolong survival. In dogs, the vector-derived myotubularin level in skeletal muscles was also variable and, in general, higher in the infused limb. In dog 4, where differences between the infused and noninfused limbs were more pronounced, functional reconstitution was observed even in muscles where myotubularin was barely detectable and the pathology was not fully corrected. In the other two dogs, dogs 5 and 6, the levels of myotubularin were higher in all muscles (30 to 140% as measured in biopsies) and led to an objectively better phenotypic correction in the whole body. Respiratory function was normalized in all three dogs. Lower than normal levels of myotubularin are therefore sufficient to ameliorate muscle function even in the presence of incomplete restoration of the histology, and a dose of ~2×10^{13} vg/kg was fully therapeutic in both animal models of the disease. Even though comparing doses in different studies is a difficult exercise, the results of a recent clinical study on the systemic administration of an AAV8 vector expressing human factor IX in hemophilia B patients suggest that a dose of 10^{13} vg/kg may be administrable to XLMTM patients, possibly in combination with transient immunosuppression (*4*, *37*).

In contrast to previous observations in animal models of DMD (*24*, *38*), our data demonstrate relatively long-term expression of AAV-derived myotubularin in muscles of XLMTM mice and dogs treated with a single dose of recombinant vector. A major difference between DMD and XLMTM is that the pathology of myotubularin-deficient muscles is not per se associated with inflammation or with the cycles of degeneration/regeneration typical of dystrophic muscles (*13*, *15*, *39*). The correction of pathology observed for XLMTM is unlikely to occur in the advanced stages of dystrophic myopathies like DMD, where muscle fibers degenerate and are irreversibly replaced by fat and fibrotic tissue. Notably, we observed no humoral response against MTM1 or cellular immune response against either the vector or MTM1, highlighting major differences in the vector-host interactions in the case of nondystrophic muscle pathology. Normal skeletal myofibers are long-lived, and transgene expression can persist up to 10 years in human skeletal muscle after AAV-mediated gene transfer (*40*). We can therefore predict that in the absence of inflammatory, humoral, or cytotoxic immune responses, vector-derived MTM1 expression could persist for many years in muscles of XLMTM patients treated by gene therapy. The presence of residual levels of myotubularin, as observed in the canine animal model, will probably be a decisive factor in limiting the risk of adverse immune reactions.

In conclusion, our results demonstrate that intravenous AAV8-mediated gene therapy leads to long-term systemic correction of XLMTM in small- and large-animal models at doses compatible with clinical application, and pave the way to a clinical trial of gene therapy for myotubular myopathy.

MATERIALS AND METHODS

Study design

Predefined study components. Preliminary data indicated that six animals were required in each group to detect a 20% difference in muscle strength with 80% power, and an α of 0.05. No animals were excluded from analysis.

Rationale and design of study. This was an early-stage observational study designed to search for possible differences among experimental treatment (gene replacement) groups. Animals were assigned to treatment groups on the basis of availability of gene replacement vector. For mouse experiments, the primary endpoint was survival; for dogs, the primary endpoint was muscle strength.

Randomization and blinding. This was an open-label and non-randomized study. For dogs, functional data were analyzed by an investigator (J.A.D.) blinded to the intervention.

Replication. Repeated functional measures were conducted over time in animals as indicated. Technical replicates were performed in PCR, Western blot, and immunological assays.

Animals

Mice were handled according to French and European legislation on animal care and experimentation and approved by the institutional ethical committee. The constitutive KO of the myotubularin gene (KO-*Mtm1*, also named BS53d4-129pas) was described previously (*13*, *18*). Wild-type littermate males were used as controls.

Dogs were handled according to principles outlined in the National Institutes of Health (NIH) *Guide for the Care and Use of Laboratory Animals*. XLMTM dogs were described previously (*15*). Affected males were identified by PCR-based genotyping, as described.

Construction and production of AAV8-*MTM1* vectors

The recombinant adeno-associated virus vector AAV2/8-pDesmin-*Mtm1*^{murine} (designated AAV8-*Mtm1*) was constructed as follows. Murine *Mtm1* cDNA [AF073996, National Center for Biotechnology Information (NCBI)] was cloned downstream of the human desmin promoter in the AAV2 expression plasmid pAAV2-pDes by PCR amplification. Pseudotyped recombinant AAV2/8 viral preparations were generated by packaging AAV2-inverted terminal repeat recombinant genomes into AAV8 capsids using a tritransfection protocol as previously described (*17*). Viral titers were quantified by a TaqMan real-time PCR assay (Applied Biosystems) and expressed as viral genomes per milliliter (vg/ml).

The recombinant adeno-associated virus vector AAV2/8-pDesmin-*MTM1*^{canine} containing a canine myotubularin cDNA regulated by the desmin promoter (designated AAV8-c*MTM1*) was produced in a baculovirus/Sf9 system (*41*). Two baculovirus batches were generated: one expressing *rep* and *cap* AAV genes and the second bearing the canine *MTM1* cDNA (XM850116, NCBI) downstream from the human desmin promoter. The AAV8-c*MTM1* vector particles were produced after baculoviral double infection of insect Sf9 cells and purified from total cell culture with AVB affinity chromatography column (GE Healthcare, AVB Sepharose high performance). The concentration in vg/ml was determined from deoxyribonuclease-resistant particles by a TaqMan real-time PCR assay (Applied Biosystems). Other routine quality control assays for recombinant AAV vectors were performed, including sterility and purity tests.

Administration of AAV8-*MTM1* vectors

Systemic vector administration in mice. AAV8-*Mtm1* at 3×10^{13} vg/kg was injected into the tail vein of 3- and 5-week-old KO-*Mtm1* mice. An equivalent volume of saline was administrated to either KO-*Mtm1* or wild-type animals as controls.

Intramuscular delivery in dogs. AAV8-c*MTM1* (4×10^{11} vg) diluted in 1 ml of lactated Ringer's solution was injected under ultrasound guidance into the midbelly of the cranial tibialis muscle of one hindlimb of unvaccinated 10-week-old affected male XLMTM dogs under anesthesia. The cranial tibialis muscle of the contralateral limb was injected with an equal volume of Ringer's solution alone. Unaffected male littermates (wild type) received 1 ml of Ringer's solution in each hindlimb.

High-pressure intravascular limb infusion. In anesthetized XLMTM dogs, AAV8-c*MTM1* (2.5×10^{13} vg/kg) diluted in PBS was infused into the distal saphenous vein under pressure (300 torr) against a tourniquet as described (*42*). Briefly, a tourniquet was positioned at the level of the groin and adjusted until the femoral pulse was no longer detectable by ultrasound, to transiently block blood inflow to the target limb. Vector was suspended in PBS at 20% of the total hindlimb volume (determined by water volume displacement) and administered via a 14-gauge catheter placed into a distal branch of the peripheral saphenous vein on the dorsum of the paw. The tourniquet was tightened for a total of 15 min (10 min before and 5 min during the infusion). In each dog, one hindlimb was infused with vector, whereas the contralateral hindlimb was not infused. For vector copy and immunoblot analysis, the midsection of the muscle belly was sampled at biopsy or necropsy.

VCN analysis

The number of vector genomes per diploid genome was quantified from 80 ng of total DNA by TaqMan real-time PCR with a 7900 HT thermocycler (Applied Biosystems). The canine β glucuronidase gene was used for standardization. The primers and probe used for vector genome (*MTM1*) amplification were as follows: 5′-ATAAGTTTTGGACATAAGTTTGC-3′ (forward), 5′-CATTTGCCATACACAATCAA-3′ (reverse), and 5′-CGACGCTGACCGGTCTCCTA-3′ (probe). The primers and probe used for β glucuronidase amplification were as follows: 5′-ACGCTGATTGCTCACACCAA-3′ (forward), 5′-CCCCAGGTCTGCTTCATAGTTG-3′ (reverse), and 5′-CCCGGCCCGTGACCTTTGTGA-3′ (probe) (Applied Biosystems).

Quantitative immunoblot analysis

Several muscle cryosections of 30 μm each (300 μm to 1 mm in total) were sliced, and proteins were extracted and analyzed by SDS–polyacrylamide gel electrophoresis and Western blotting as previously described (*16*). Membranes were probed with either a polyclonal antibody against the C-terminal part of murine myotubularin [R2348 (*17*)] or a rabbit polyclonal antibody raised against the C terminus of canine myotubularin (R1040, Généthon). A mouse monoclonal antibody specific for GAPDH (Millipore, MAB374) was used as internal control. Detection was performed with a secondary antibody coupled to IRDye 680 (LI-COR) and the Odyssey infrared imaging system (LI-COR Biotechnology Inc.).

Histological and immunofluorescence analyses

Histology and morphometry. For mouse studies, cryosections (7 μm) of frozen muscles were processed for H&E and NADH-TR stainings using standard procedures. The proportion of internalized nuclei and the diameter of myofibers were quantified as previously described (*16*).

For canine studies, serial 8-μm-thick transverse cryosections were prepared from frozen muscles and processed for H&E and NADH-TR stainings. The number of centrally nucleated fibers and fibers with mislocalization of organelles (including mitochondrial aggregates and necklace fibers) was quantified manually from photographs taken at ×200 magnification. For fiber size quantification, muscles were immunostained as described above with rabbit anti-dystrophin antibodies (Abcam PLC, ab15277) and Alexa Fluor–conjugated anti-rabbit IgG (Molecular Probes). Staining was evaluated, and MinFeret diameters of fibers were quantified with a Nikon Eclipse 90i microscope with NIS-Elements AR software (Nikon Instruments Inc.) and a BX53 microscope and cellSens Standard software (Olympus). Slides for evaluation of canine cardiac

pathology were produced through the Children's Research Institute Histology Core Facility at Medical College of Wisconsin (MCW). Electron microscopy was performed at MCW's Electron Microscopy Core Facility, and quantification of sarcotubular structures was performed as described previously (*35*).

Immunofluorescence. For immunostaining of muscle tissue, frozen transverse sections were fixed for 10 min by incubation in PBS at 100°C. Nonspecific antigens were blocked with PBS, 0.2% Tween, and 3% bovine serum albumin at room temperature. Sections were then incubated at 4°C overnight with mouse primary antibodies directed against DHPR1α (Thermo Scientific Pierce, MA3-920) or dysferlin (Novocastra, NCL-HAMLET). After extensive PBS washes, sections were incubated with biotinylated goat anti-mouse antibodies (SouthernBiotech) and, after additional washes, with streptavidin conjugated with Alexa Fluor 488 (Invitrogen). Glass slides were mounted with FluorSave reagent (Calbiochem, Merck) and visualized with a Leica confocal microscope TCS-SP2. Digital images of a slice corresponding to the muscle midsection were acquired with a charge-coupled device camera (Sony) and a motorized stage.

Muscle function

Muscle function in mice.

Actimeter test. Spontaneous locomotor activity in mice was assessed with the LE 8811 IR motor activity monitor (Bioseb). Briefly, mice were placed in an open field bounded with 16 horizontal photoelectric infrared beams to measure three-dimensional movements of the animals. The distance crossed was recorded and analyzed for 90 min.

Escape test. Global strength of mice was evaluated as previously described (*43*). Measurements of isometric contractile properties of murine extensor digitorum longus muscles were performed in vitro as published (*17*).

Hindlimb contraction in dogs

Contractile properties in canine muscles in vivo were assessed as previously described (*19*, *20*). Briefly, the hindlimb torque of anesthetized dogs was measured by wrapping the foot to a pedal mounted on the shaft of a servomotor that also functioned as a force transducer. Percutaneous stimulation of the peroneal nerve activated hindlimb muscles to pull the foot up toward the body to generate torque. Isometric contractions were performed over a range of stimulation frequencies to determine torque-frequency relationships, and investigators blinded to the experimental treatment analyzed the data.

Diaphragm muscle function in dogs

PIF was assessed under anesthesia by pneumatography as previously described (*44*). Briefly, airflow was measured before the administration of the centrally acting stimulant doxapram chloride (1.0 mg/kg) and again after respiratory increase. Raw tracings were visually examined to ensure complete capture of each breath before computer analysis. Ten clear and successive breaths were selected from those collected at baseline and again at the respiratory peak.

Statistical analysis

Statistical analyses were performed with SAS software (version 6; SAS Institute Inc.). Individual means were compared with nonparametric tests (Mann-Whitney, or Wilcoxon rank-sum and two-sided *t* tests). Differences were considered to be statistically significant at $P < 0.05$ (*), $P < 0.01$ (**), or $P < 0.001$ (***). All data are presented as means ± SEM unless stated otherwise.

SUPPLEMENTARY MATERIALS

www.sciencetranslationalmedicine.org/cgi/content/full/6/220/220ra10/DC1

Immune response profile in XLMTM dogs

Fig. S1. Pathology of muscles from myotubularin-deficient mice at 3 weeks of age.

Fig. S2. Systemic gene replacement therapy ameliorates pathological hallmarks of myotubular myopathy in skeletal muscles.

Fig. S3. Intravascular delivery of a lower dose of AAV8-*Mtm1* in myotubularin-deficient mice improves partially life span and body growth.

Fig. S4. Targeted myotubularin gene replacement therapy in XLMTM dogs increases the overall size of injected muscles.

Fig. S5. Targeted gene therapy with AAV8-*MTM1* injected into the cranial tibialis muscle improves in vivo contractile response to repeated lengthening (eccentric) contractions in XLMTM dogs.

Fig. S6. In vivo strength measured 1 year after regional hindlimb infusion of AAV8-*MTM1* in an XLMTM dog.

Fig. S7. Representative Western blot of myotubularin transgene expression in XLMTM dogs infused with AAV8-*MTM1*.

Fig. S8. Necropsy findings in the heart of an XLMTM dog 1 year after AAV8-*MTM1* infusion.

Fig. S9. Humoral response specific to AAV8 and myotubularin in XLMTM dogs.

Fig. S10. Cellular response to AAV8 or MTM1 protein in XLMTM dogs.

Table S1. Quantified histological findings in dogs after intramuscular injection.

Table S2. Quantified histological findings in dogs after intravenous AAV.

Table S3. Quantified histological findings in autopsy tissue at 1 year after infusion.

Table S4. Innate immune responses after intramuscular or regional limb administration of AAV8-*MTM1* in XLMTM dogs (dogs 1 to 6) and an untreated XLMTM dog (dog C).

Movie S1. Wild-type mouse (red tail) and myotubularin-deficient mouse (blue tail) treated with AAV8-*Mtm1* (3×10^{13} vg/ml) at 6 months after injection (note the robust appearance, normal size, and activity of the treated *Mtm1* KO mouse).

Movie S2. XLMTM dogs (dogs 4 to 6) treated with AAV8-*MTM1*, two untreated XLMTM dogs, and a normal control dog at various times.

REFERENCES AND NOTES

1. A. M. Maguire, F. Simonelli, E. A. Pierce, E. N. Pugh Jr., F. Mingozzi, J. Bennicelli, S. Banfi, K. A. Marshall, F. Testa, E. M. Surace, S. Rossi, A. Lyubarsky, V. R. Arruda, B. Konkle, E. Stone, J. Sun, J. Jacobs, L. Dell'Osso, R. Hertle, J. X. Ma, T. M. Redmond, X. Zhu, B. Hauck, O. Zelenaia, K. S. Shindler, M. G. Maguire, J. F. Wright, N. J. Volpe, J. W. McDonnell, A. Auricchio, K. A. High, J. Bennett, Safety and efficacy of gene transfer for Leber's congenital amaurosis. *N. Engl. J. Med.* **358**, 2240–2248 (2008).
2. J. W. Bainbridge, A. J. Smith, S. S. Barker, S. Robbie, R. Henderson, K. Balaggan, A. Viswanathan, G. E. Holder, A. Stockman, N. Tyler, S. Petersen-Jones, S. S. Bhattacharya, A. J. Thrasher, F. W. Fitzke, B. J. Carter, G. S. Rubin, A. T. Moore, R. R. Ali, Effect of gene therapy on visual function in Leber's congenital amaurosis. *N. Engl. J. Med.* **358**, 2231–2239 (2008).
3. J. Bennett, M. Ashtari, J. Wellman, K. A. Marshall, L. L. Cyckowski, D. C. Chung, S. McCague, E. A. Pierce, Y. Chen, J. L. Bennicelli, X. Zhu, G. S. Ying, J. Sun, J. F. Wright, A. Auricchio, F. Simonelli, K. S. Shindler, F. Mingozzi, K. A. High, A. M. Maguire, AAV2 gene therapy readministration in three adults with congenital blindness. *Sci. Transl. Med.* **4**, 120ra115 (2012).
4. A. C. Nathwani, E. G. Tuddenham, S. Rangarajan, C. Rosales, J. McIntosh, D. C. Linch, P. Chowdary, A. Riddell, A. J. Pie, C. Harrington, J. O'Beirne, K. Smith, J. Pasi, B. Glader, P. Rustagi, C. Y. Ng, M. A. Kay, J. Zhou, Y. Spence, C. L. Morton, J. Allay, J. Coleman, S. Sleep, J. M. Cunningham, D. Srivastava, E. Basner-Tschakarjan, F. Mingozzi, K. A. High, J. T. Gray, U. M. Reiss, A. W. Nienhuis, A. M. Davidoff, Adenovirus-associated virus vector-mediated gene transfer in hemophilia B. *N. Engl. J. Med.* **365**, 2357–2365 (2011).
5. J. R. Mendell, L. R. Rodino-Klapac, X. Q. Rosales, B. D. Coley, G. Galloway, S. Lewis, V. Malik, C. Shilling, B. J. Byrne, T. Conlon, K. J. Campbell, W. G. Bremer, L. E. Taylor, K. M. Flanigan, J. M. Gastier-Foster, C. Astbury, J. Kota, Z. Sahenk, C. M. Walker, K. R. Clark, Sustained alpha-sarcoglycan gene expression after gene transfer in limb-girdle muscular dystrophy, type 2D. *Ann. Neurol.* **68**, 629–638 (2010).
6. J. R. Mendell, K. Campbell, L. Rodino-Klapac, Z. Sahenk, C. Shilling, S. Lewis, D. Bowles, S. Gray, C. Li, G. Galloway, V. Malik, B. Coley, K. R. Clark, J. Li, X. Xiao, J. Samulski, S. W. McPhee, R. J. Samulski, C. M. Walker, Dystrophin immunity in Duchenne's muscular dystrophy. *N. Engl. J. Med.* **363**, 1429–1437 (2010).

7. S. Herson, F. Hentati, A. Rigolet, A. Behin, N. B. Romero, F. Leturcq, P. Laforet, T. Maisonobe, R. Amouri, H. Haddad, M. Audit, M. Montus, C. Masurier, B. Gjata, C. Georger, M. Cherai, P. Carlier, J. Y. Hogrel, A. Herson, Y. Allenbach, F. M. Lemoine, D. Klatzmann, H. L. Sweeney, R. C. Mulligan, B. Eymard, D. Caizergues, T. Voit, O. Benveniste, A phase I trial of adeno-associated virus serotype 1-γ-sarcoglycan gene therapy for limb girdle muscular dystrophy type 2C. *Brain* **135**, 483–492 (2012).
8. D. E. Bowles, S. W. McPhee, C. Li, S. J. Gray, J. J. Samulski, A. S. Camp, J. Li, B. Wang, P. E. Monahan, J. E. Rabinowitz, J. C. Grieger, L. Govindasamy, M. Agbandje-McKenna, X. Xiao, R. J. Samulski, Phase 1 gene therapy for Duchenne muscular dystrophy using a translational optimized AAV vector. *Mol. Ther.* **20**, 443–455 (2012).
9. H. Jungbluth, C. Wallgren-Pettersson, J. Laporte, Centronuclear (myotubular) myopathy. *Orphanet. J. Rare Dis.* **3**, 26 (2008).
10. J. Laporte, L. J. Hu, C. Kretz, J. L. Mandel, P. Kioschis, J. F. Coy, S. M. Klauck, A. Poustka, N. Dahl, A gene mutated in X-linked myotubular myopathy defines a new putative tyrosine phosphatase family conserved in yeast. *Nat. Genet.* **13**, 175–182 (1996).
11. J. Laporte, F. Blondeau, A. Buj-Bello, D. Tentler, C. Kretz, N. Dahl, J. L. Mandel, Characterization of the myotubularin dual specificity phosphatase gene family from yeast to human. *Hum. Mol. Genet.* **7**, 1703–1712 (1998).
12. F. L. Robinson, J. E. Dixon, Myotubularin phosphatases: Policing 3-phosphoinositides. *Trends Cell Biol.* **16**, 403–412 (2006).
13. A. Buj-Bello, V. Laugel, N. Messaddeq, H. Zahreddine, J. Laporte, J. F. Pellissier, J. L. Mandel, The lipid phosphatase myotubularin is essential for skeletal muscle maintenance but not for myogenesis in mice. *Proc. Natl. Acad. Sci. U.S.A.* **99**, 15060–15065 (2002).
14. J. J. Dowling, A. P. Vreede, S. E. Low, E. M. Gibbs, J. Y. Kuwada, C. G. Bonnemann, E. L. Feldman, Loss of myotubularin function results in T-tubule disorganization in zebrafish and human myotubular myopathy. *PLOS Genet.* **5**, e1000372 (2009).
15. A. H. Beggs, J. Böhm, E. Snead, M. Kozlowski, M. Maurer, K. Minor, M. K. Childers, S. M. Taylor, C. Hitte, J. R. Mickelson, L. T. Guo, A. P. Mizisin, A. Buj-Bello, L. Tiret, J. Laporte, G. D. Shelton, *MTM1* mutation associated with X-linked myotubular myopathy in Labrador Retrievers. *Proc. Natl. Acad. Sci. U.S.A.* **107**, 14697–14702 (2010).
16. R. Joubert, A. Vignaud, M. Le, C. Moal, N. Messaddeq, A. Buj-Bello, Site-specific *Mtm1* mutagenesis by an AAV-Cre vector reveals that myotubularin is essential in adult muscle. *Hum. Mol. Genet.* **22**, 1856–1866 (2013).
17. A. Buj-Bello, F. Fougerousse, Y. Schwab, N. Messaddeq, D. Spehner, C. R. Pierson, M. Durand, C. Kretz, O. Danos, A. M. Douar, A. H. Beggs, P. Schultz, M. Montus, P. Denèfle, J. L. Mandel, AAV-mediated intramuscular delivery of myotubularin corrects the myotubular myopathy phenotype in targeted murine muscle and suggests a function in plasma membrane homeostasis. *Hum. Mol. Genet.* **17**, 2132–2143 (2008).
18. L. Al-Qusairi, N. Weiss, A. Toussaint, C. Berbey, N. Messaddeq, C. Kretz, D. Sanoudou, A. H. Beggs, B. Allard, J. L. Mandel, J. Laporte, V. Jacquemond, A. Buj-Bello, T-tubule disorganization and defective excitation-contraction coupling in muscle fibers lacking myotubularin lipid phosphatase. *Proc. Natl. Acad. Sci. U.S.A.* **106**, 18763–18768 (2009).
19. J. N. Kornegay, D. J. Bogan, J. R. Bogan, M. K. Childers, D. D. Cundiff, G. F. Petroski, R. O. Schueler, Contraction force generated by tarsal joint flexion and extension in dogs with golden retriever muscular dystrophy. *J. Neurol. Sci.* **166**, 115–121 (1999).
20. M. K. Childers, R. W. Grange, J. N. Kornegay, In vivo canine muscle function assay. *J. Vis. Exp.* e2623 (2011).
21. R. W. Grange, J. Doering, E. Mitchell, M. N. Holder, X. Guan, M. Goddard, C. Tegeler, A. H. Beggs, M. K. Childers, Muscle function in a canine model of X-linked myotubular myopathy. *Muscle Nerve* **46**, 588–591 (2012).
22. L. T. Su, K. Gopal, Z. Wang, X. Yin, A. Nelson, B. W. Kozyak, J. M. Burkman, M. A. Mitchell, D. W. Low, C. R. Bridges, H. H. Stedman, Uniform scale-independent gene transfer to striated muscle after transvenular extravasation of vector. *Circulation* **112**, 1780–1788 (2005).
23. A. Toromanoff, Y. Chérel, M. Guilbaud, M. Penaud-Budloo, R. O. Snyder, M. E. Haskins, J. Y. Deschamps, L. Guigand, G. Podevin, V. R. Arruda, K. A. High, H. H. Stedman, F. Rolling, I. Anegon, P. Moullier, C. Le Guiner, Safety and efficacy of regional intravenous (r.i.) versus intramuscular (i.m.) delivery of rAAV1 and rAAV8 to nonhuman primate skeletal muscle. *Mol. Ther.* **16**, 1291–1299 (2008).
24. A. Vulin, I. Barthélémy, A. Goyenvalle, J. L. Thibaud, C. Beley, G. Griffith, R. Benchaouir, M. le Hir, Y. Unterfinger, S. Lorain, P. Dreyfus, T. Voit, P. Carlier, S. Blot, L. Garcia, Muscle function recovery in golden retriever muscular dystrophy after AAV1-U7 exon skipping. *Mol. Ther.* **20**, 2120–2133 (2012).
25. A. Goyenvalle, J. T. Seto, K. E. Davies, J. Chamberlain, Therapeutic approaches to muscular dystrophy. *Hum. Mol. Genet.* **20**, R69–R78 (2011).
26. J. P. Greelish, L. T. Su, E. B. Lankford, J. M. Burkman, H. Chen, S. K. Konig, I. M. Mercier, P. R. Desjardins, M. A. Mitchell, X. G. Zheng, J. Leferovich, G. P. Gao, R. J. Balice-Gordon, J. M. Wilson, H. H. Stedman, Stable restoration of the sarcoglycan complex in dystrophic muscle perfused with histamine and a recombinant adeno-associated viral vector. *Nat. Med.* **5**, 439–443 (1999).
27. P. Gregorevic, M. J. Blankinship, J. M. Allen, R. W. Crawford, L. Meuse, D. G. Miller, D. W. Russell, J. S. Chamberlain, Systemic delivery of genes to striated muscles using adeno-associated viral vectors. *Nat. Med.* **10**, 828–834 (2004).
28. P. Gregorevic, M. J. Blankinship, J. M. Allen, J. S. Chamberlain, Systemic microdystrophin gene delivery improves skeletal muscle structure and function in old dystrophic mdx mice. *Mol. Ther.* **16**, 657–664 (2008).
29. K. Inagaki, S. Fuess, T. A. Storm, G. A. Gibson, C. F. Mctiernan, M. A. Kay, H. Nakai, Robust systemic transduction with AAV9 vectors in mice: Efficient global cardiac gene transfer superior to that of AAV8. *Mol. Ther.* **14**, 45–53 (2006).
30. Z. Wang, R. Storb, C. L. Halbert, G. B. Banks, T. M. Butts, E. E. Finn, J. M. Allen, A. D. Miller, J. S. Chamberlain, S. J. Tapscott, Successful regional delivery and long-term expression of a dystrophin gene in canine muscular dystrophy: A preclinical model for human therapies. *Mol. Ther.* **20**, 1501–1507 (2012).
31. Z. Fan, K. Kocis, R. Valley, J. F. Howard, M. Chopra, H. An, W. Lin, J. Muenzer, W. Powers, Safety and feasibility of high-pressure transvenous limb perfusion with 0.9% saline in human muscular dystrophy. *Mol. Ther.* **20**, 456–461 (2012).
32. V. R. Arruda, H. H. Stedman, V. Haurigot, G. Buchlis, S. Baila, P. Favaro, Y. Chen, H. G. Franck, S. Zhou, J. F. Wright, L. B. Couto, H. Jiang, G. F. Pierce, D. A. Bellinger, F. Mingozzi, T. C. Nichols, K. A. High, Peripheral transvenular delivery of adeno-associated viral vectors to skeletal muscle as a novel therapy for hemophilia B. *Blood* **115**, 4678–4688 (2010).
33. Z. Li, E. Colucci, C. Babinet, D. Paulin, The human desmin gene: A specific regulatory programme in skeletal muscle both in vitro and in transgenic mice. *Neuromuscul. Disord.* **3**, 423–427 (1993).
34. B. J. Byrne, D. J. Falk, N. Clément, C. S. Mah, Gene therapy approaches for lysosomal storage disease: Next-generation treatment. *Hum. Gene Ther.* **23**, 808–815 (2012).
35. M. W. Lawlor, D. Armstrong, M. G. Viola, J. J. Widrick, H. Meng, R. W. Grange, M. K. Childers, C. P. Hsu, M. O'Callaghan, C. R. Pierson, A. Buj-Bello, A. H. Beggs, Enzyme replacement therapy rescues weakness and improves muscle pathology in mice with X-linked myotubular myopathy. *Hum. Mol. Genet.* **22**, 1525–1538 (2013).
36. C. R. Pierson, A. N. Dulin-Smith, A. N. Durban, M. L. Marshall, J. T. Marshall, A. D. Snyder, N. Naiyer, J. T. Gladman, D. S. Chandler, M. W. Lawlor, A. Buj-Bello, J. J. Dowling, A. H. Beggs, Modeling the human *MTM1* p.R69C mutation in murine *Mtm1* results in exon 4 skipping and a less severe myotubular myopathy phenotype. *Hum. Mol. Genet.* **21**, 811–825 (2012).
37. F. Mingozzi, K. A. High, Immune responses to AAV vectors: Overcoming barriers to successful gene therapy. *Blood* **122**, 23–36 (2013).
38. M. Le Hir, A. Goyenvalle, C. Peccate, G. Précigout, K. E. Davies, T. Voit, L. Garcia, S. Lorain, AAV genome loss from dystrophic mouse muscles during AAV-U7 snRNA-mediated exon-skipping therapy. *Mol. Ther.* **21**, 1551–1558 (2013).
39. N. Romero, Centronuclear myopathies: A widening concept. *Neuromuscul. Disord.* **20**, 223–228 (2010).
40. G. Buchlis, G. M. Podsakoff, A. Radu, S. M. Hawk, A. W. Flake, F. Mingozzi, K. A. High, Factor IX expression in skeletal muscle of a severe hemophilia B patient 10 years after AAV-mediated gene transfer. *Blood* **119**, 3038–3041 (2012).
41. R. H. Smith, J. R. Levy, R. M. Kotin, A simplified baculovirus-AAV expression vector system coupled with one-step affinity purification yields high-titer rAAV stocks from insect cells. *Mol. Ther.* **17**, 1888–1896 (2009).
42. M. Petrov, A. Malik, A. Mead, C. R. Bridges, H. H. Stedman, Gene transfer to muscle from the isolated regional circulation. *Methods Mol. Biol.* **709**, 277–286 (2011).
43. C. Carlson, R. Makiejus, A noninvasive procedure to detect muscle weakness in the mdx mouse. *Muscle Nerve* **13**, 480–484 (1990).
44. M. A. Goddard, E. L. Mitchell, B. K. Smith, M. K. Childers, Establishing clinical end points of respiratory function in large animals for clinical translation. *Phys. Med. Rehabil. Clin. N. Am.* **23**, 75–94 (2012).

Acknowledgments: We thank F. Barnay-Toutain, Y. Garnier, B. Gjata, J. Marchant, A. Menuet, K. Pappante, T. Savic, D. Stockholm, J. Tan, and P. Veron for help with the experiments; K. Block and M. Lockard for clinical support; M. Holder for help with canine experiments and clinical support; and A. Atala, C. Le Guiner, and J.-L. Mandel for support and/or discussions. **Funding:** Association Française contre les Myopathies (France) to A.B.-B. and M.K.C.; Muscular Dystrophy Association (United States) to M.K.C. and A.H.B.; Myotubular Trust (UK) to A.B.-B.; Genopole d'Evry (France) to A.B.-B.; INSERM (France) to A.B.-B.; Région d'Alsace (France) to T.J.; U.S. NIH grants P50 NS040828 and R01 AR044345 to A.H.B., K08 AR059750 to M.W.L., and R21 AR064503 and R01 HL115001 to M.K.C.; Anderson Family Foundation to A.H.B.; Joshua Frase Foundation to A.H.B. and M.K.C.; and Where There's a Will There's a Cure and Peter Khuri Myopathy Research Foundation to M.K.C.
Author contributions: M.K.C., M.E.F., R.W.G., M.W.L., C. Masurier, F.M., P.M., A.H.B., and A.B.-B. participated in the study design. For the canine studies, M.K.C., R.W.G., X.G., M.G., and E.M. carried out physiological assays and T.S., K.P., and J.A.D. analyzed image and/or myograph data. M.W.L. performed histopathological studies. E.M. and J.B. provided breeding and animal care oversight. K.P. and C. Masurier performed vector biodistribution, immunoblots, immunohistochemistry, and other immunological assays. R.J., C. Moal, T.J., K.P., N.D., C.H., and L.V.W.

performed mouse studies. S.M. and C.R. produced AAV vectors. M.K.C., R.W.G., M.W.L., A.V., C. Masurier, F.M., P.M., A.H.B., and A.B.-B. reviewed some or all of the primary data. M.K.C., M.E.F., F.M., and A.B.-B. wrote the manuscript. All authors reviewed the manuscript. **Competing interests:** M.K.C. is a paid member of the Scientific Advisory Board of Audentes Therapeutics and holds stock options in this company. A.H.B. is a paid member of the Scientific Advisory Board of Audentes Therapeutics. M.L. consults for AVI Therapeutics and Sarepta Therapeutics. M.K.C., A.H.B., and A.B.-B. are coauthors of a patent on AAV8 gene therapy for treating myotubular myopathy filed by Wake Forest University (U.S. Provisional Patent Application No. 61/771,449, filed 1 March 2013, "Systemic gene replacement therapy for treatment of XLMTM"). The other authors declare that they have no competing interests.

Submitted 5 September 2013
Accepted 2 January 2014
Published 22 January 2014
10.1126/scitranslmed.3007523

Citation: M. K. Childers, R. Joubert, K. Poulard, C. Moal, R. W. Grange, J. A. Doering, M. W. Lawlor, B. E. Rider, T. Jamet, N. Danièle, S. Martin, C. Rivière, T. Soker, C. Hammer, L. Van Wittenberghe, M. Lockard, X. Guan, M. Goddard, E. Mitchell, J. Barber, J. K. Williams, D. L. Mack, M. E. Furth, A. Vignaud, C. Masurier, F. Mavilio, P. Moullier, A. H. Beggs, A. Buj-Bello, Gene therapy prolongs survival and restores function in murine and canine models of myotubular myopathy. *Sci. Transl. Med.* **6**, 220ra10 (2014).